Validation of satellite-constrained ammonia using a CTM and ground measurements

Nikolaos Evangeliou[1,*], Yves Balkanski[2], Sabine Eckhardt[1], Anne Cozic[2], Didier Hauglustaine[2], Andreas Stohl[1]

[1]Norwegian Institute for Air Research (NILU), Department of Atmospheric and Climate Research (ATMOS), Kjeller, Norway.
[2]Laboratoire des Sciences du Climat et de l'Environnement (LSCE), CEA-CNRS-UVSQ, 91191, Gif-sur-Yvette, France.

The Research Council of Norway

EGU European Geosciences Union

More Info here

INTRODUCTION

Ammonia (NH3) has received a lot of attention nowadays due to its impact on the population and the environment (Erisman, 2004). In the troposphere, it reacts with the abundant sulphuric and nitric acids (Malm, 2004) contributing up to 50 % of the total mass of PM2.5 and PM10 at some regions (Anderson et al., 2003). Due to the secondary PM formation, ammonia alters human health (Gu et al., 2014) causing premature mortality. It has also a climate impact, as ammonium particles affect Earth's radiative balance. Sources of ammonia include wild animals, watersheds, traffic), sewage systems, humans, biomass burning, volcanic eruptions and agriculture (Erisman et al., 2007) (*Figure 1*). The latter is responsible for the majority of the global atmospheric emissions of ammonia. Emissions have increased considerably since pre-industrial times and are unlikely to decrease due to the growing demand for food and feed (Aneja et al., 2008).

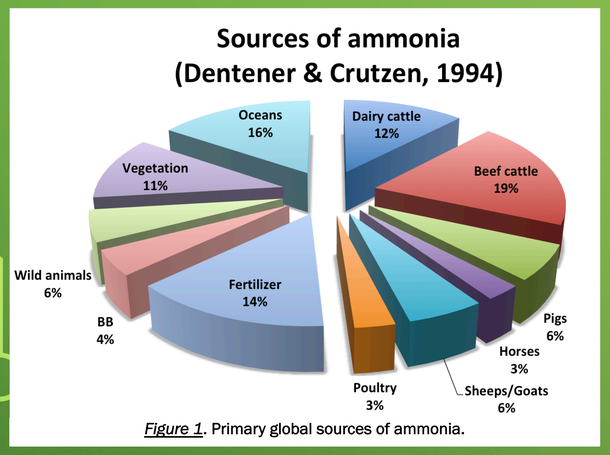


Figure 1. Primary global sources of ammonia.

Despite its importance, ammonia is one of the most poorly quantified trace gases, with errors over 50% on the global emission budget and even higher on temporal and local scales (Dentener and Crutzen, 1994). In the present study we use 10 years (2008–2017) of satellite measurements of ammonia retrieved from IASI to calculate surface emissions. The calculated emissions are then ingested in a Chemistry Transport Model (CTM) and simulated for the same 10–year period. To verify the improvement of the calculated emissions of ammonia, we evaluate the modelled surface concentrations against ground–based measurements from different monitoring stations. The same comparison is performed for the most recent state–of–the–art emission dataset.

FLUX CALCULATIONS OF AMMONIA

Emission fluxes of ammonia were calculated using a 1–dimensional box model that assumes first-order loss terms for ammonia (Van Damme et al., 2018). It takes into account the gridded column IASI concentrations and the removal processes of ammonia in a hypothetical atmospheric box following the next equation:

$$E_{NH3} = {M_{NH3}}/{\tau}$$

where M_{NH_3} is the mass of ammonia in each grid-cell (in molecules cm^{-2}) and τ is the lifetime of ammonia in the box (given in seconds).

The IASI measurements were set into a 2-dimensional grid of 0.5°×0.5° using an Inverse Distance Weighting (IDW) method (Renka, 1988) preferred for its ease of use and high quality of interpolation.

The lifetime of ammonia is highly variable, due to the chemical loss and deposition processes that affect it. To tackle this problem, instead of using a constant value, we calculated gridded lifetimes from a CTM. This gives robustness in the calculated fluxes; e.g., at regions where sulfuric and nitric acids are abundant, chemical loss will be more effective and, thus, lifetime much shorter affecting fluxes.

In a CTM, lifetime of ammonia can be easily calculated by the species mass balance equation (Croft et al., 2014):

$$\frac{dC(t)}{dt} = S(t) - \frac{C(t)}{\tau(t)}$$

where $C(t)$ is the atmospheric burden of ammonia at time t, $S(t)$ is the time-dependent source emission fluxes and $\tau(t)$ is the removal timescale. Assuming steady-state conditions and continuous fluxes, there is a quasi-equilibrium between sources and removals of ammonia and the modelled aerosol lifetime τ_{mod} can be written as:

$$\tau_{mod} = {C_{NH3}}/{L_{NH3}^{trans,chem,depo}}$$

where C_{NH3} is the atmospheric burden of ammonia and $L_{NH3}^{trans,chem,depo}$ is the total loss due to any process affecting ammonia in the model (transport, chemical loss, dry deposition).

RESULTS & DISCUSSIONS

Lifetime of ammonia is in the order of a few hours to a few days (Behera et al., 2013), thus ammonia can be only transported over short distances as (a) the majority of its emissions occur at the surface, and (b) it presents high deposition velocities for most surfaces (Hov et al., 1994). Lifetime depends on numerous factors such as the presence of ammonia's reactants, atmospheric water vapour, and temperature, atmospheric mixing and advection and emissions. At ammonia–poor conditions, all ammonia is rapidly removed by neutralising sulfuric acid. If ammonia increases further (ammonia–rich conditions), then reaction with nitric acid occurs forming nitric ammonium. If sulfate concentrations decrease, then free ammonia is produced, which gradually reacts with nitric acid producing aerosol phase nitric ammonium. But if particles are aqueous, then the sulfates in the solution increase the equilibrium vapour pressure of ammonia with nitric acid reversing the reaction towards the gaseous phase reactants. So, sulfate reductions are linked with non-linear increases of aerosol nitrates and decreases of aerosol ammonium and water (Seinfeld and Pandis, 2000).

The modelled lifetimes of ammonia are shown in *Figure 2*. The average lifetime was calculated to be 11.6 ± 0.6 hours, which is in the range of the previously reported values. The lowest values (~10 hours) were observed in clean remote areas characterized by low ammonia emissions (Central America, Sahara and Australia), while in the rest of the globe the lifetime was close to the average. The highest lifetimes (~16 hours) were calculated for Southern Brazil and Venezuela, which are both areas with relatively high ammonia emissions and low concentrations of sulfuric and nitric acid, which both affect the fast removal of ammonia fast increasing its lifetime.

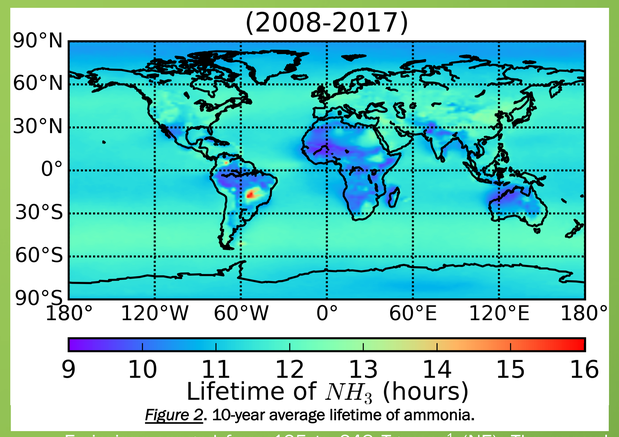


Figure 2. 10-year average lifetime of ammonia.

Emissions ranged from 195 to 248 Tg $year^{-1}$ (NE). The annual emissions reported by Van Damme et al. (2018) (VD0.5) were 186 Tg, which are comparable with the average of the 10-year period in NE (average $\pm$ *sd*: 216 ± 19 Tg $year^{-1}$). NE emissions were also compared with emissions calculated from Van Damme et al. (2018) gridded IASI column data applying the variable (modelled) lifetimes of ammonia (*Figure 2*) (VDgrlf). The latter showed a better agreement with the NE emissions with mean annual different of 14±19 Tg $year^{-1}$ (average±sd).

VD0.5, VDgrlf and NE emissions were much higher than traditional emissions such as those of ECLIPSE5-GFED4-GEIA (EGG) and EDGAR4.3.1-GFED4. Specifically, the 10-year average difference of NE emissions from ECLIPSE5-GFED4-GEIA (EGG) was 150 ± 19 Tg $year^{-1}$, while somehow lower (109 ± 18 Tg $year^{-1}$) from the most updated EDGAR4.3.1-GFED. At the same time, the average difference of NE emissions from VD0.5 was only 29 ± 18 Tg $year^{-1}$.

Figure 3 illustrates hot-spot regions of ammonia (Europe, North America, South America and Southeastern Asia) from NE together with their seasonal variation. Total emissions of ammonia over Europe were estimated as 15±2 Tg $year^{-1}$, more than double compared with those reported in EGG (6.9±1.1 Tg $year^{-1}$) and similar to those reported in VD0.5 (11 Tg $year^{-1}$) or those in VDgrlf (11±1.0 Tg $year^{-1}$). No obvious seasonality can be seen for Europe as a whole, as the hot-spot regions are rather few. An exception in years 2010 and 2015 was observed with a late summer peak due to emissions in the Po valley, the most intense industrial and agricultural region of Italy. In North America, hot-spot regions can be easily distinguished. First, a small region in Colorado, Central US (agricultural region), Iowa (animal farming), northern Texas and Kansas (beef cattle), and southern Idaho (dairy cattle), Also, the three major valleys in Salt Lake, Cache, and Utah (pig farms) and the San Joaquin Valley in California (animals). Annual emissions in North America were estimated to be 1.1±0.1 Tg $year^{-1}$. Maximum emissions were observed in late spring, due to the contribution from mineral fertilizer and manure application and in summer, due to influence of livestock housing emissions. In S.America the largest fluxes were observed from August to October, due to biomass burning. NE emissions were 28±3 Tg $year^{-1}$ close to VD0.5 (22 Tg $year^{-1}$) and VDgrlf (24±1.3 Tg $year^{-1}$) and four times higher than EGG (7.1±0.3 Tg $year^{-1}$). SE Asia is the largest agricultural contributor in the global ammonia budget. Emissions peak in late summer, when emissions from rice cultivation, synthetic fertilizer application and livestock manure spreading persist and in spring when wheat cultivation dominates. NE emissions were 38±2 Tg $year^{-1}$ similar to VD0.5 (36 Tg $year^{-1}$) and VDgrlf (39±1.8 Tg $year^{-1}$) and slightly higher than EGG (25±1.2 Tg $year^{-1}$).

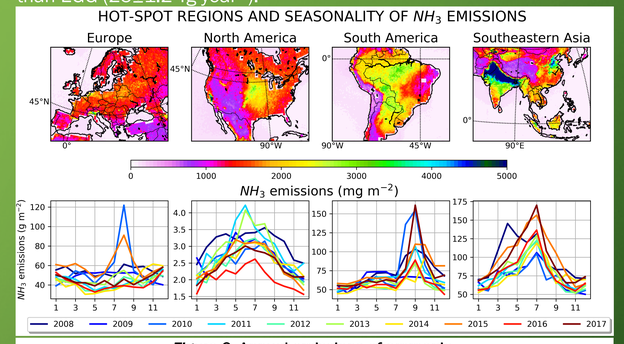


Figure 3. Annual emissions of ammonia.

To validate the calculated emissions of ammonia, we compared modelled concentrations against measurements from EMEP (https://emep.int/mscw/), EANET (https://www.eanet.asia) and AMoN (http://nadp.slh.wisc.edu/data/AMoN/). (*Figure 4*).. Ammonia was simulated using the LMDzORINCA model that includes full chemistry of the N cycle (Hauglustaine et al., 2014) using NE, VD0.5, VDgrlf and EGG emissions. All emission datasets underestimated concentrations of ammonia over Europe. The most accurate prediction was achieved using NE emissions that gave small underestimations (-72%) and RMSEs, while 80% of the concentrations were less than 10 times from the observations. In N. America, VD0.5 and VDgrlf emissions gave better results than the other datasets considering the calculated biases, RMSEs and the fact that more than 95% of the predicted concentrations fell within the 10-fold limit from the 1×1 line. In SE Asia, all emissions inventories underestimated station concentrations of EANET with bias between -98% (EGG) and -47% (VD0.5). The least spread concentrations were those simulated using VD0.5 and VDgrlf (smallest RMSEs) also having the largest fraction within the 10-fold limit (95%).

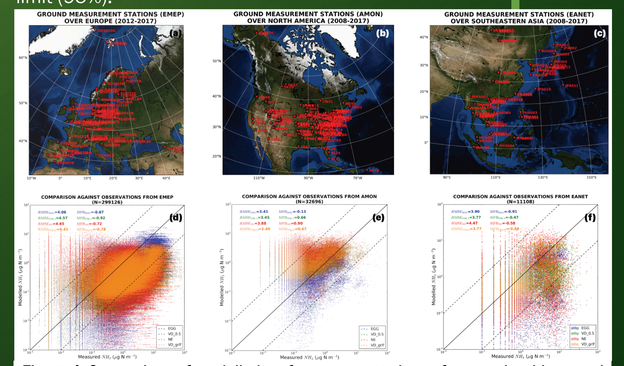


Figure 4. Comparison of modelled surface concentrations of ammonia with ground measurements from EMEP.

REFERENCES

Anderson et al. (2003), doi:10.1016/S0160-4120(02)00186-1; Aneja et al. (2008), 10.1038/ngeo236; Behera et al. (2013), doi:10.1007/s11356-013-2051-9; Croft et al. (2014), doi:10.5194/acp-14-4313-2014; Dentener and Crutzen (1994), doi:10.1007/bf00694492; Erisman (2004), doi:10.1641/0006-3568(2004)054[0286:TNDOMO]2.0.CO;2; Erisman et al. (2007), doi:10.1016/j.envpol.2007.06.033; Gu et al. (2014), doi:10.1890/14.WB.007; Hauglustaine et al. (2014), doi:10.5194/acp-14-11031-2014; Hov et al. (1994), doi:10.1029/94jd00910; Malm (2004), doi:10.1029/2003JD003739; Renka (1988), doi:10.1145/45054.45055; Seinfeld and Pandis (2000), John Wiley & Sons, NY.; Van Damme et al. (2018), doi:10.1038/s41586-018-0747-1;